International Communications in Heat and Mass Transfer 88 (2017) 228–235

Contents lists available at ScienceDirect

International Communications in Heat and Mass Transfer

journal homepage: www.elsevier.com/locate/ichmt

A comparative study on the performances of different shell-and-tube type latent heat thermal energy storage units including the effects of natural convection

Guang-Shun Han[a,b], Hong-Sheng Ding[a], Yun Huang[b], Li-Ge Tong[c,*], Yu-Long Ding[d]

[a] School of Mathematics and Physics, University of Science and Technology Beijing, Beijing 100083, China
[b] State Key Laboratory of Multiphase Complex Systems, Institute of Process Engineering, Chinese Academy of Sciences, Beijing 100190, China
[c] School of Energy and Environmental Engineering, University of Science and Technology Beijing, Beijing 100083, China
[d] Birmingham Centre for Thermal Energy Storage, University of Birmingham, Birmingham B152TT, United Kingdom

ARTICLE INFO

Keywords:
Natural convection
Latent heat storage
Pipe model
Cylinder model
PCM

ABSTRACT

Numerical modeling was performed to simulate the melting process of a fixed volume/mass phase-change material (PCM) in different shell-and-tube type latent thermal energy storage units with identical heat transfer area. The effect of liquid PCM natural convection (NC) on the latent heat storage performance of the pipe and cylinder models was investigated using a 3D numerical model with FLUENT software. Result shows that NC can cause a non-uniform distribution of the solid–liquid interface, which accelerates PCM melting rate. The PCM melting rate and heat storage rate in the horizontal cylinder model are higher than those in the horizontal pipe model because of the combined effects of heat conduction and NC. A comparative study was conducted to determine the effects of horizontal and vertical shell-and-tube models with different heat transfer fluid (HTF) inlets including the effects of NC. The results indicate that the vertical model with an HTF inlet at the bottom exhibits the highest PCM melting rate and heat storage rate for the pipe models. For the cylinder models, the horizontal model and the vertical model with an HTF inlet at the bottom can achieve nearly the same completed melting time. In addition, NC has minimal effect on any model with an HTF inlet at the top.

1. Introduction

Thermal energy storage plays an important role in energy conservation and in the development of new energy sources. This type of storage can resolve energy mismatch caused by time and space conflicts, as well as improve the reliability of energy supply systems. Among available thermal energy storage technologies, latent heat thermal energy storage (LHTES) based on phase-change materials (PCMs) exhibits considerable advantages such as high thermal energy density and a nearly constant phase transition temperature. LHTES has great potential for harvesting solar energy and recovering industrial heat waste [1–4]. However, most inexpensive PCMs exhibit low thermal conductivity that reduces latent heat storage performance. Thus, enhancing heat transfer capability is one of the objectives of this research.

In recent years, shell-and-tube heat exchangers with high efficiency and simple architecture have been extensively used in LHTES. Many numerical and experimental studies have been performed on this subject. Two models are used in most of these experimental and numerical studies. In the first model (designated as the pipe model), a PCM fills in the shell side and the heat transfer fluid (HTF) flows through a single tube [5–8]. In the second model (designated as the cylinder model), a PCM fills in the tube and the HTF flows parallel to the tube [9,10,11]. Both can have either horizontal or vertical configurations to match thermal storage system [12,13,14]. In many numerical and experimental models, natural convection (NC) is an important factor that should be considered, particularly when a mobile phase, such as a melting PCM, is involved in the process. NC occurs in the melt layer and generally increases heat transfer rate. The possible role of NC in heat transfer has been explored to a certain degree in numerical and experimental studies. Sparrow et al. [15] experimentally investigated the heat transfer behavior during the PCM melting process in a vertical tube. A significant difference was observed between the experimentally determined values and those predicted by modeling, possibly because of considerable volume changes and the occurrence of NC in the liquid phase. Hosseini et al. [16] experimentally and numerically investigated the effect of NC on the melting process of PCM inside a shell and tube heat exchanger. A sharp increase in temperature occurred at the

* Corresponding author.
E-mail address: tonglige@me.ustb.edu.cn (L.-G. Tong).

http://dx.doi.org/10.1016/j.icheatmasstransfer.2017.09.009

uppermost section of the heat storage unit within the melt layer. Darzi et al. [17] developed a 2D mathematical model of a shell-and-tube PCM system and studied the melting process in cylinders arranged in concentric and eccentric arrays. The position of the inner cylindrical tube was varied to investigate the melting of PCM-filled shells. The predicted results showed that the melting rate was approximately the same for concentric and eccentric arrays during the initial stage. After a certain period, the melting rate decreased in the concentric array, whereas the melting rate curve became nearly linear in the eccentric arrays. Yazici et al. [18] experimentally investigated the solidification behavior of PCM in a horizontal shell-and-tube LHTES system. Five positions with different eccentricities with respect to the outer shell were studied. The results indicated that total solidification time increased regardless of whether the center of the inner tube was upward or downward. Dhaidan et al. [19] performed experimental and numerical investigations on the melting behavior of a nano-sized PCM inside an annular cavity formed between two circular cylinders. The acceleration of the melting rate by NC was more significant when the concentration of nanoparticles was relatively low.

For the pipe and cylinder models, many experimental and numerical studies have been performed with regard to enhancing latent heat storage performance with NC, as described in the literature review. However, minimal research has been conducted to compare the performances of pipe and cylinder models and to make a comprehensive inquiry on the effects of horizontal and vertical configurations. The objective of the present study is to evaluate the effect of NC on the melting of PCM in a pipe model and a cylinder model with the same volume/mass of PCM and heat transfer area. In addition, a comparative study was performed among horizontal and vertical models with different HTF inlets. The effects of NC on PCM melting rate, solid–liquid interface, heat storage rate, and total energy storage capacity were investigated.

2. Physical and numerical models

2.1. Physical model

The physical models of two shell-and-tube LHTES units are shown in Fig. 1. The length of the pipe and cylinder models (L_p/L_c) is 500 mm, and the radii of the inner and outer tubes are 10 mm and 14.14 mm ($R_o = \sqrt{2}\, R_i$), respectively. The thickness of the tube walls is neglected, which can satisfy the same volume/mass of PCM and heat transfer area. Different HTF inlets, in accordance with the horizontal and vertical configurations, are incorporated into two shell-and-tube units in six cases, as shown in Fig. 2. The cases are summarized in Table 1.

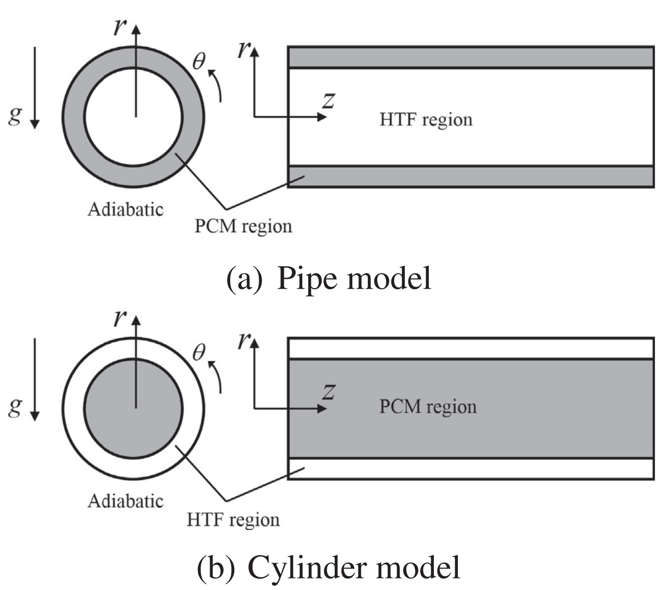

Fig. 1. Physical models of the two shell-and-tube LHTES units.

Only the charging process, which is PCM melting, is investigated in present study. The PCM used is solar salt, which is a eutectic mixture of potassium nitrate (60wt% KNO_3) and sodium nitrate (40 wt% $NaNO_3$), and air is employed as HTF. The thermophysical properties of the PCM and the HTF are provided in Table 2. The specific heat (C_p) and thermal conductivity (k) of the HTF are obtained as polynomial functions of temperature among these parameters [20]. In the simulation, the initial temperature of both the PCM and the HTF is set to 393 K, which is lower than the phase change temperature of the PCM. The inlet temperature and inlet velocity of the HTF is kept constant at 573 K and 15 m/s, respectively.

Half of the shell-and-tube units can be chosen as the computational domain based on axial symmetry. To simplify the mathematical domain, the following assumptions and approximations for the models are made.

(1) The PCM is homogeneous and isotropic.
(2) Axial heat conduction and viscous dissipation in the HTF are negligible, and HTF flow is regarded as a fully developed, dynamic laminar flow.
(3) The thickness of the inner and outer tube walls is negligible, and the outer tube wall is regarded as an adiabatic boundary.
(4) The thermophysical properties of PCM are independent of temperature, and the thermal conductivity and specific heat of the HTF change with temperature, as shown in Table 2.

2.2. Governing equations

In the present study, the solidification/melting model with NC that uses a computational fluid dynamics software is adopted to simulate the 3D melting process of PCM. Enthalpy measurement is performed to study the movement of the solid–liquid interface in the PCM. Based on the aforementioned assumptions and approximations, HTF flow is considered a 1D fluid flow. The governing equations are as follows:

For the HTF,

$$\frac{\partial \theta_f}{\partial t} = -\frac{m_f}{\rho_f \pi {R_i}^2}\frac{\partial \theta_f}{\partial z} - \frac{2U}{(\rho c_p)_f R_i}(\theta_f - \theta_p{}^*), \tag{1}$$

where $\theta_f = T_f - T_m$, T_f is the HTF temperature, $\theta_p{}^*$ is the PCM temperature at $r = R_i$, and U is the local convection heat transfer coefficient of the HTF, which can be calculated by the following correlation [21].

$$U = \frac{Nu{\cdot}k}{d} = \frac{k}{d} \times 0.022 \times \mathrm{Pr}^{0.6}\mathrm{Re}^{0.8} \tag{2}$$

For the PCM,
the continuity equation is

$$\frac{\partial \rho}{\partial t} + \frac{1}{r}\frac{\partial (r\rho u)}{\partial r} + \frac{1}{r}\frac{\partial (\rho v)}{\partial \theta} + \frac{\partial (\rho w)}{\partial z} = 0. \tag{3}$$

The momentum equations are

$$\begin{aligned}\rho\frac{\partial u}{\partial t} + \rho\frac{u}{r}\frac{\partial u}{\partial \theta} + \rho v\frac{\partial u}{\partial r} + \rho w\frac{\partial u}{\partial z} \\ = -\frac{\partial p}{\partial \omega} + \eta\left(\frac{1}{r^2}\frac{\partial^2 u}{\partial \theta^2} + \frac{1}{r}\frac{\partial}{\partial r}\left(r\frac{\partial u}{\partial r}\right) + \frac{\partial^2 u}{\partial z^2}\right) + \frac{1}{r^2}\frac{\partial u}{\partial \theta} - \rho\frac{uv}{r} - \eta\frac{u}{r^2} \\ + g_\theta,\end{aligned} \tag{4}$$

$$\begin{aligned}\rho\frac{\partial v}{\partial t} + \rho\frac{u}{r}\frac{\partial v}{\partial \theta} + \rho v\frac{\partial v}{\partial r} + \rho w\frac{\partial v}{\partial z} \\ = -\frac{\partial p}{\partial r} + \eta\left(\frac{1}{r^2}\frac{\partial^2 v}{\partial \theta^2} + \frac{1}{r}\frac{\partial}{\partial r}\left(r\frac{\partial v}{\partial r}\right) + \frac{\partial^2 v}{\partial z^2}\right) - \frac{1}{r^2}\frac{\partial u}{\partial \theta} + \rho\frac{u^2}{r} - \eta\frac{v}{r^2} + g_r,\end{aligned} \tag{5}$$